

**16th International Conference on  
Harmonisation within Atmospheric Dispersion Modelling for Regulatory Purposes  
8-11 September 2014, Varna, Bulgaria**

---

**PARAMETRIZING LOW-FREQUENCY MESOSCALE MOTIONS IN ATMOSPHERIC  
DISPERSION MODELS**

*Helen Webster, Thomas Whitehead and David Thomson<sup>1</sup>*

<sup>1</sup>Met Office, UK

**Abstract:** To accurately predict plume spread and air concentrations, unresolved motions need to be represented in atmospheric dispersion models. Here we use spectral analysis techniques to propose a suitable parametrization for low-frequency mesoscale motions not resolved by the input NWP model. Velocity variances and timescales of the missing motions in the NWP model data are quantified. We analyse how these parameters vary with input NWP data of different resolutions and between the boundary layer and the free troposphere.

**Key words:** *plume meander, unresolved motions, parametrization, spectral analysis, stable light wind conditions*

## INTRODUCTION

Large variations in wind direction have been observed in stable light wind conditions. This variation in wind direction is due to two-dimensional horizontal eddies which often cause plume meandering. These motions are not usually resolved by the meteorological data used to drive atmospheric dispersion models nor are they covered by parametrizations of small-scale three-dimensional turbulent motions. The representation of these mesoscale motions in atmospheric dispersion models is particularly important in stable light wind conditions when they are the dominant cause of lateral plume spread. It has been shown that neglecting these intermediate scale motions leads to underestimation of plume spread (Gupta et al., 1997) and overestimation of air concentrations (Maryon, 1998). Indeed Kristensen et al. (1981) suggest that estimates of mean concentrations can be at least factors of 4 - 6 too high if these motions are not taken into account.

## PARAMETRIZING LOW-FREQUENCY MESOSCALE MOTIONS

Low-frequency horizontal wind components are parametrized within the Met Office's atmospheric dispersion model NAME (Numerical Atmospheric-dispersion Modelling Environment (Jones et al., 2007)) using random walk techniques analogous to those used to model random turbulent motions. This technique is dependent on obtaining appropriate values for velocity variances and Lagrangian timescales.

Webster and Thomson (2005) studied the spectral gap between Numerical Weather Prediction (NWP) resolved motions and the turbulence parametrization. Energy spectra of the resolved motions were generated from time-series of NWP wind components ( $u$  and  $v$ ). The spectra obtained from NWP data were compared to spectra obtained from near-surface observational data.

A discrete Fourier transform

$$u_m = \sum_{q=-(N/2-1)}^{N/2} A_q \cos\left(\frac{2\pi qm}{N}\right) + \sum_{q=-(N/2-1)}^{N/2-1} B_q \sin\left(\frac{2\pi qm}{N}\right), \quad (1)$$

was calculated using fast Fourier transform routines, where  $u_m$  is the time-series of wind components ( $u$  or  $v$ ),  $A_q$  and  $B_q$  are the Fourier components

$$A_q = \frac{1}{N} \sum_{n=1}^N u_n \cos\left(\frac{2\pi qn}{N}\right), \quad q = \pm 1, \pm 2, \dots, \pm\left(\frac{N}{2} - 1\right)$$

$$B_q = \frac{1}{N} \sum_{n=1}^N u_n \sin\left(\frac{2\pi qn}{N}\right), \quad q = \pm 1, \pm 2, \dots, \pm\left(\frac{N}{2} - 1\right)$$

$$A_0 = \frac{1}{N} \sum_{n=1}^N u_n,$$

$$A_{N/2} = \frac{1}{N} \sum_{n=1}^N u_n \cos(n\pi),$$

and  $N$  is the number of data points in the time-series. The total variance is given by

$$\langle (u_m - \langle u_m \rangle)^2 \rangle = \langle u_m^2 \rangle - \langle u_m \rangle^2 = \sum_{q=1}^{N/2-1} 2(A_q^2 + B_q^2) + A_{N/2}^2.$$

The variance at each wavenumber,  $q$ , namely

$$2(A_q^2 + B_q^2), \quad q = 1, \dots, N/2 - 1$$

$$A_{N/2}^2, \quad q = N/2$$

is multiplied by  $N\Delta t$ , where  $\Delta t$  is the time interval between  $u_m$  and  $u_{m+1}$ , and plotted against the frequency,  $f$ , where  $f = q/(N\Delta t)$ . Hence the highest frequency represented is given by  $f = 1/(2\Delta t)$  and the area under the plotted spectral curve gives the total variance. The raw spectral curve is noisy and hence a block averaging method is applied, in which the frequency boundaries of the blocks increase by roughly a factor of 4/3 between blocks (i.e., the number of data values to be averaged increases by approximately a factor of 4/3 from one block to the next).

#### VARIATIONS WITH DIFFERENT NWP INPUT DATA

In recent years, advances in computing and NWP modelling have led to the development of high resolution NWP models with spatial resolutions of the order of 1-2 km. With this advancement comes the expectation that smaller scale atmospheric motions will be resolved by the NWP model. The resulting parametrization of unresolved low-frequency mesoscale motions, designed to fill the spectral gap between the resolved motions and the parametrization of small-scale three-dimensional turbulent motions, is therefore likely to depend on the input NWP model resolution.

To understand how the parametrization of low-frequency mesoscale motions should vary with input NWP data of different temporal and spatial resolutions, the missing variance between the observed and NWP spectra was calculated using data from a range of configurations of the Met Office's NWP model, the 'Unified Model', with different model resolutions. Figure 1 compares the spectra generated from observed wind data and from NWP model winds at a height of 10m for two sites during 2012. At Wattisham (52.12°N, 0.96°E) hourly spot observations are available, whereas at Cardington (52.10°N, 0.42°W) wind observations every 10 minutes are available. The higher time resolution of the Cardington observations enables the energy spectra to be calculated out to higher frequencies. In both cases the observed spectra contains more energy than the NWP model spectra at high frequencies. Furthermore, the resolution (temporal and spatial) of the NWP model has a significant effect on capturing motions at high frequencies, with the global model (25km horizontal resolution with the wind data used here interpolated from 3-hourly data) having more missing energy than the other models of higher temporal and spatial resolution (NAE model - 12km resolution, hourly data; 4km model - 4km resolution, hourly data; UKV model - 1.5km resolution, hourly data). Appropriate velocity variances for the parametrization of missing low-frequency mesoscale motions can be found by calculating the area between the observed and NWP model spectra.

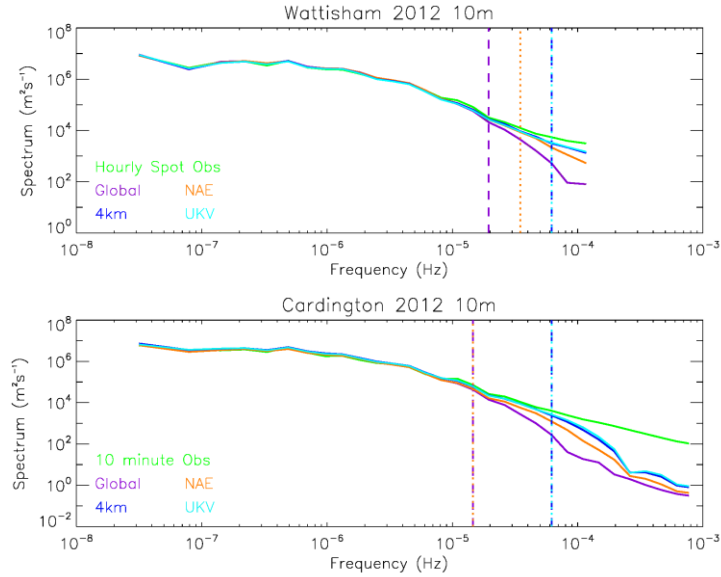
The parametrization of low-frequency mesoscale motions also requires appropriate timescales. The correlation between  $u$  at two times ( $s$  and  $s + t$ ) is assumed to take the form

$$R(t) = \frac{\overline{u(s)u(s+t)}}{\sigma_u^2} = \exp\left(\frac{-t}{\tau}\right),$$

where  $\tau$  is the integral timescale. To obtain a timescale for the missing motions, a fast Fourier transform is applied to the observed and NWP time series of wind components. The energy spectra ( $\varphi = A_q^2 + B_q^2$ ) is calculated from the Fourier components ( $A_q$  and  $B_q$ ) for  $q=0, \pm 1, \pm 2, \dots, \pm(N/2-1), N/2$  and filtered to remove the low frequency motions by setting the spectra ( $A_q^2 + B_q^2$ ) to zero for wavenumbers  $q=0, \pm 1, \pm 2, \dots, \pm(D-1)$  where  $f=D/(N\Delta t)$  is the frequency at which the modelled spectra diverges from the observed spectra. The difference between the filtered spectra obtained from observations and the filtered spectra obtained from NWP model data is calculated and an inverse Fourier transform ( $F^{-1}$ ) applied to give the correlation function ( $R_m$ ) for only the highest frequency motions of interest,

$$R_m = F^{-1}[\phi(obs) - \phi(mod)]_{filtered},$$

where  $m=0, \dots, N-1$ . Plotting  $R_m$  against  $t=m\Delta t$ , one can determine a timescale for the missing motions from the time at which the correlation first falls to  $1/e$  of its initial value ( $R_0$ ). The velocity variances ( $\sigma_u^2$ ) can also be determined by this method and are given by the initial value of the correlation function ( $R_0$ ).



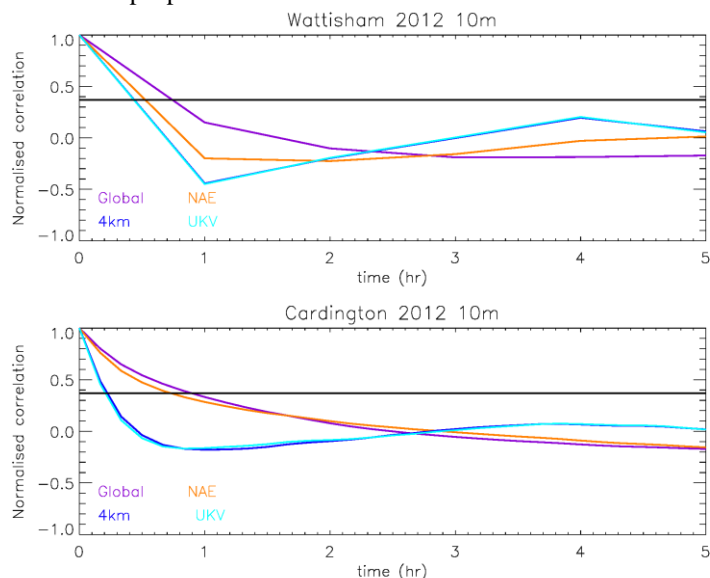
**Figure 1.** A comparison of near-surface energy spectra generated from observed and NWP model 10m wind data.

Figure 2 shows the correlation functions (normalised by the variance) for the motions corresponding to the missing energy in the NWP spectra shown in Figure 1. The higher resolution NWP models have the smallest predicted timescales. The timescale determined by this method, using wind data at a fixed point in space, is an Eulerian timescale ( $\tau_E$ ); the Lagrangian timescale ( $\tau_L$ ) is generally larger than the Eulerian timescale. Pasquill and Smith (1983) and Hanna (1981) discuss the relationship between Eulerian and Lagrangian timescales for turbulence. There is some scatter in the ratio  $\tau_L / \tau_E = \beta$  obtained from observations. Here we use  $\beta = 3$  to determine a Lagrangian timescale from the calculated Eulerian timescale, noting, however, that there is some uncertainty in this  $\beta$  value.

## PARAMETRIZING LOW-FREQUENCY MESOSCALE MOTIONS WITHIN THE FREE TROPOSPHERE

Most parametrizations of unresolved low-frequency mesoscale motions are based on wind observations within the boundary layer. In comparison the free troposphere is not well understood and the applicability of the same boundary layer parametrizations within the free troposphere is questionable. The spectral method presented here requires long time-series of frequent wind observations at a fixed point. Obtaining such a high quality and lengthy dataset at elevations above the boundary layer is far from trivial. Powerful

wind profilers provide regular observations at heights above the boundary layer and are therefore well suited to investigate the free troposphere.



**Figure 2.** Normalised correlation functions for the missing motions in the NWP model spectra. The  $1/e$  line (shown) is used to determine the timescale.

Observations from a network of wind profilers located around the UK have been used in the spectral analysis of missing motions in NWP data in the free troposphere. The smaller wind profilers routinely measure up to a height of around 3 km, whereas the largest and most powerful wind profilers routinely measure up to a height of around 16 km. Large and powerful wind profilers are located at Aberystwyth (52.42°N, 4.01°W) and South Uist (57.25°N, 7.38°W) and both routinely observe the atmosphere above the boundary layer. Figure 3 shows a comparison of spectra generated from 30-minute wind profiler observations and from NWP model wind data at a sample height within the free troposphere at these two sites. The corresponding normalised filtered correlation functions representing the missing motions in the NWP data are given in Figure 4.

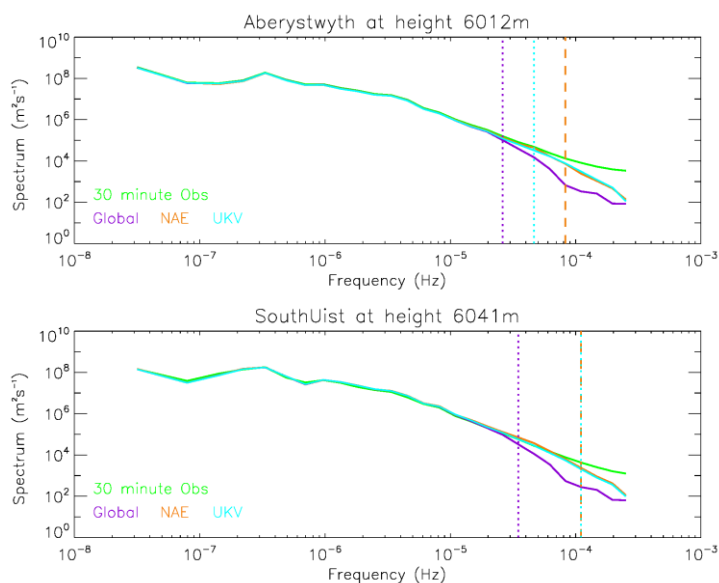


**Figure 3.** A comparison of free-tropospheric energy spectra generated from wind profiler observations and NWP model wind data.

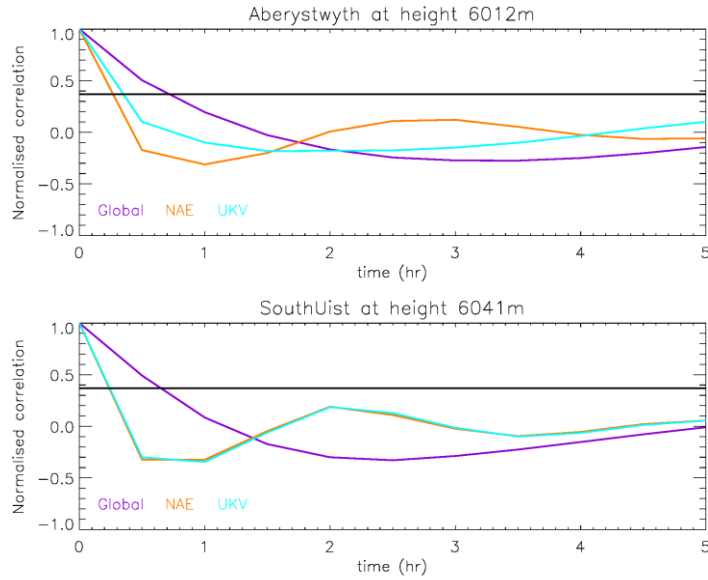


**Figure 4.** Normalised correlation functions for the missing motions in the NWP model spectra within the free troposphere.

There is more energy at all scales of motion in the free troposphere (compare the vertical axis in Figures 1 and 3), indicative of higher wind speeds aloft. The NWP model spectra appear to diverge from the observations spectra at a higher frequency for data within the free troposphere. The temporal resolution of the NWP model data seems to be the dominating factor in representing atmospheric motions of certain scales at these altitudes, with the spatial resolution of the NWP models assessed here having little impact within the free troposphere.

## RESULTS AND DISCUSSION

The frequency at which the observed and NWP model spectra are deemed to have diverged is identified. The missing variance ( $\sigma^2$ ) between the observed and NWP model spectra from this point of divergence to the high frequency end of the spectra is calculated. A timescale ( $\tau_E$ ) is also calculated from the correlation function, filtered based on this point of divergence. A diffusivity value ( $K$ ) is then obtained from the calculated velocity variances and Lagrangian timescales ( $K = \sigma^2 \tau_L = 3\sigma^2 \tau_E$ ). The point of divergence is chosen based on a 30% difference between the observed and NWP model spectra and is indicated by the vertical lines in Figures 1 and 3.

Results do show some dependence on the method chosen to determine the point of divergence. Furthermore there is some variation in results between different observing sites, instrumentation, observing altitudes and for different time resolutions of the observations. Nonetheless, there is consistent evidence that the diffusivities used in the parametrization of low-frequency mesoscale motions should depend on the resolution of the input NWP data with larger diffusivities employed with lower resolution models. There is less evidence to indicate that a different parameterisation should be used within the free troposphere, with greater variations between different observing sites than between the boundary layer and the free troposphere. (In particular, the Aberystwyth wind profiler data results in much larger diffusivities than data from the other wind profiler sites.) Table 1 summarises the range of diffusivities obtained using recent near-surface and free tropospheric observations at different altitudes and at various UK locations. The time resolution of the observations ranges from 10 minutes to an hour. The diffusivity values indicated by this work are mostly lower than those currently employed in NAME (currently  $K \sim 9000 \text{ m}^2 \text{ s}^{-1}$ ). This suggests that, in general, there is currently too much diffusion in NAME, although to some extent using extra diffusion can be regarded as a valid user choice intended to smooth out unpredictable features. There is a need to assess further the effect in NAME of reducing diffusion due to low-frequency mesoscale motions.

**Table 1.** A summary of diffusivities ( $K$  in  $\text{m}^2 \text{s}^{-1}$ ). (BL = boundary layer, FT = free troposphere)

<b>BL or FT</b>	<b>Temporal resolution</b>	<b>Height range (m)</b>	<b>Global (3-hourly, 25 km)</b>	<b>NAE (hourly, 12 km)</b>	<b>4km (hourly, 4 km)</b>	<b>UKV (hourly, 1.5 km)</b>
BL	hourly	10	4905 – 7245	1783 – 4947	752 – 3131	701 – 3873
	30 min	10 – 50	6550 – 8767	1890 – 5739	424 – 637	237 – 300
	10 min	10 – 50	6369 – 8543	2827 – 5423	753 – 944	609 – 832
FT	30 min	2200 – 6000	5248 – 22102	407 – 2963		243 – 4614
	10 min	2200 – 2800	7662 – 17088	1652 – 2789		1469 – 4233

## REFERENCES

- Gupta, S., R.T. McNider, M. Trainer, R.J. Zamora, K. Knupp and M.P. Singh, 1997: Nocturnal wind structure and plume growth rates due to inertial oscillations. *J. Appl. Meteorol.*, **36**, 1050-1063.
- Jones, A.R., D.J. Thomson, M. Hort and B. Devenish, 2007: The U.K. Met Office's next-generation atmospheric dispersion model, NAME III, in *Borrego, C. and A.-L. Norman (Eds) Air Pollution Modeling and its Application XVII (Proceedings of the 27th NATO/CCMS International Technical Meeting on Air Pollution Modelling and its Application)*, Springer, 580-589.
- Hanna, S.R., 1981: Lagrangian and Eulerian time-scale relations in the daytime boundary layer. *J. Appl. Meteorol.*, **20**, 242-249.
- Kristensen, L., N.O. Jensen and E.L. Peterson, 1981: Lateral dispersion of pollutants in a very stable atmosphere - The effect of meandering. *Atmos. Environ.*, **15**, 837-844.
- Maryon, R.H., 1998: Determining cross-wind variance for low frequency wind meander. *Atmos. Environ.*, **32**, 115-121.
- Pasquill, F. and F.B. Smith, 1983: Atmospheric diffusion. A study of the dispersion of windborne material from industrial and other sources, 3<sup>rd</sup> Edition, Ellis Horwood Limited, Chichester, UK, 437 pp.
- Webster, H.N. and D.J. Thomson, 2005: Parameterising low-frequency meander in atmospheric dispersion models, in *Skouloudis, A.N., P. Kassomenos and J. Bartzis (Eds) Tenth International Conference on Harmonisation within Atmospheric Dispersion Modelling for Regulatory Purposes*, 594-598.